Adsorption (2008) 14: 171–179
DOI 10.1007/s10450-007-9060-2

Comparative features of ar adsorption on smooth and amorphous surfaces examined by density functional theory

E.A. Ustinov

Received: 28 April 2007 / Revised: 30 July 2007 / Accepted: 24 September 2007 / Published online: 16 October 2007

Abstract We analyze argon adsorption isotherms and isosteric heat of adsorption on graphitized and nongraphitized carbon black and silica surfaces by means of nonlocal density functional theory (NLDFT). It is shown that in the case of graphitized carbon black the behavior of the adsorbed phase is nearly identical to that in the bulk phase at a distance larger than about 3-4 molecular diameters from the surface. At a smaller distance argon forms solid-like molecular layers at a temperature at least 3.5 K above the triple point, with the interlayer distance being markedly smaller than the argon collision diameter. In the case of defected or amorphous surfaces adsorbed argon is liquid-like below its triple point. Our extension of the Tarazona NLDFT to amorphous solids (NLDFT-AS) and the Kierlik and Rosinberg version of NLDFT excellently fit argon adsorption isotherms and properly predict the isosteric heat of adsorption. We showed that the surface roughness affects the calculated heat of adsorption, which allowed us to adjust the width of the diffuse zone of the nongraphitized carbon black and the silica surface.

Keywords Density functional theory · Adsorption isotherm · Heat of adsorption · Graphitized carbon black · Nongraphitized carbon black · Silica · Amorphous surface

E.A. Ustinov (✉)
Research & Production Company "Provita", 3-7, 24th Linia, St Petersburg, 199106 Russia
e-mail: eustinov@mail.wplus.net

Ioffe Physical Technical Institute, Polytechnicheskaya 26, St Petersburg, 194021 Russia

1 Introduction

The surface structure is known to substantially affect the behavior of adsorbed gases, which is reflected in adsorption isotherms and heat of adsorption. It is important to know features of the adsorbed phase to ensure the correct description of the mechanism of adsorption and its subsequent extension to adsorption in pores of different shape and characterization of porous materials. Promising results have been recently achieved using molecular approaches like Grand Canonical Monte Carlo (GCMC) simulations and nonlocal density functional theory (NLDFT). However, some substantial discrepancies between theoretical end experimental results even in such simple systems as N_2 or Ar-graphitized thermal carbon black (GTCB) still remain, indicating that the detailed mechanism of adsorption is not completely understood (Olivier et al. 1994; Ustinov and Do 2004). This motivated invoking empirical correction of the intermolecular potential induced by the GTCB surface (Olivier 1995; Ustinov and Do 2004; Do et al. 2004). Later on (Do and Do 2007) the deviation of the predicted adsorption isotherms from experimental data was attributed to polarization of adsorbed molecules by quadrupoles located on the graphite surface. In the case of N_2 or Ar adsorption on nongraphitized carbon black and silica surface, the standard NLDFT model fails to fit the experimental isotherms properly, which stimulated attempts to extent NLDFT to amorphous surfaces. Thus, we modified the Tarazona version of NLDFT to account for random spatial distribution of solid atoms and their contribution to the smoothed density near the surface (Ustinov et al., 2005, 2006, 2007). We named the developed version nonlocal density functional theory for amorphous solids (NLDFT-AS). Recently the quenched solid density functional theory (QSDFT) based on the fundamental measure theory (FMT) and the idea of the solid–fluid binary

mixture was developed for the case of adsorption on amorphous solids (Ravikovitch and Neimark 2006). Both approaches excellently describe the adsorption isotherms with no need to resort to additional energy distribution function, say, in the framework of the patchwise model, meaning that usual energetic heterogeneity of amorphous solids is embedded in the models. In order to further test the approaches, in the present paper, we compare experimental and predicted isosteric heat of argon adsorption on nongraphitized carbon black and silica surface. The ultimate goal of this paper is to characterize the state of the adsorbed argon on smooth and rough surfaces.

2 Model

The basis of density functional theory is comprehensively described in the literature. In the case of open system the fluid density distribution at a given chemical potential μ and temperature T corresponds to the minimum of grand thermodynamic potential, Ω. Since in our case, the density ρ of the gas adsorbed on the open surface is assumed to change only along the direction z normal to the surface, the condition of minimum Ω can be written as follows:

$$kT\ln[\Lambda^3\rho(z)] + \Psi[\rho(z)] + 2j(z)u[\rho(z)] + V(z) - \mu = 0 \tag{1}$$

Here $\Psi[\rho(z)] = \delta F_{ex}[\rho(z)]/\delta\rho(z)$ is the functional derivative of the excess Helmholtz free energy $F_{ex}[\rho(z)]$ with respect to local density $\rho(z)$; $u[\rho(z)]$ is the attractive intermolecular potential; $V(z)$ is the external potential exerted by the solid; Λ is the de Broglie wavelength. The correcting function $j(z)$ was introduced by Olivier (1995) to increase the description ability of NLDFT. In the standard NLDFT $j(z) = 1$ by default.

The excess Helmholtz free energy models the repulsive (reference) component of the intermolecular potential of interaction, being a function of a weighted average (smoothed) density $\overline{\rho}(z)$. The difference between different versions of NLDFT lies in the way of definition of the smoothed density and the Helmholtz free energy. In the present paper we use the Tarazona (1985) smoothed density approximation (SDA) for all types of surfaces and the Kierlik and Rosinberg (1990) NLDFT in the case of amorphous surface. The attractive component of the intermolecular potential $u[\rho(z)]$ is defined according to the conventional Weeks, Chandler, and Andersen (WCA) perturbation scheme (Weeks et al. 1971) in the framework of the mean field approximation. Following Neimark et al. (1998), we use the assumption of constant value of the equivalent hard sphere diameter d_{HS} independent of temperature. Then, because the excess Helmholtz free energy is proportional to the temperature, it contributes only to the entropy of the system. Equation (1) can be solved at a given chemical potential (or bulk pressure, p) and temperature to yield the density distribution over the adsorbed phase with an iteration procedure. Once the density distribution has been determined, one can calculate the amount adsorbed, yielding the point of the isotherm. The function $j(z)$ can be determined by the least squares fitting using Tikhonov regularization technique (Tikhonov and Arsenin 1977).

2.1 Heat of adsorption

There are two equivalent ways to determine the isosteric heat of adsorption q_{st}. The first one corresponds to the Clausius–Clapeyron equation and can be written as follows:

$$q_{st} = RT^2 Z\left(\frac{\partial \ln p}{\partial T}\right)_a \tag{2}$$

Here $Z = p/(\rho^g RT)$ is the compressibility, ρ^g is the bulk density. The derivative in the RHS of the above equation is taken at a specified amount adsorbed a. According to the second way, the heat of adsorption is determined via the partial derivative of the internal energy with respect to the amount adsorbed and can be represented as (Ustinov et al. 2006)

$$q_{st} = u^g + p/\rho^g - \int\{2j(z')u[\rho(z')] + V(z')\}\frac{\partial\rho(z')}{\partial\mu}dz' \Big/ \int\frac{\partial\rho(z')}{\partial\mu}dz' \tag{3}$$

Here u^g is the molar potential energy in the bulk phase, usually negligibly small in its absolute term. We used (3) to calculate heat of adsorption after the function $j(z)$ and the solid–fluid potential had been determined by fitting the experimental isotherm. Note that in this case we do not need experimental isotherms measured at different temperatures. In order to determine the heat of adsorption directly from experimental data, we used (2) or, assuming the linear dependence of logarithm of the pressure on the inverse temperature,

$$q_{st} \cong RT_1T_2Z\frac{\ln(p_2/p_1)}{(T_2 - T_1)} \tag{4}$$

Subscripts 1 and 2 correspond to the lower (77 K) and the higher (87.3 K) temperatures at which two adsorption isotherms were measured.

2.2 The case of amorphous solid

2.2.1 Extension of the Tarazona SDA

We extended the Tarazona SDA to the case of adsorption of gases on amorphous solids by accounting for the contribution of solid atoms to the smoothed density at a small

distance from the surface (Ustinov et al. 2005). In this case, the repulsive component of the solid–fluid potential appears as an additional increase of the Helmholtz free energy near the surface, while $V(z)$ is operated as the attractive component determined from the experimental isotherm by the least squares. Hence, the model uses similar assumptions on the fluid–fluid and solid–fluid interactions and considers the solid and the adsorbed gas as two disordered parts of a binary system from the same standpoint. It was shown (Ustinov et al., 2005, 2006, 2007) that energetic heterogeneity of the amorphous surface is naturally accounted for in the NLDFT-AS. Additionally, we introduced a structural heterogeneity (surface roughness) as a diffuse zone, where the solid density gradually changes from $\rho_0^{(s)}$ inside the solid to zero according to the error function

$$\rho^{(s)}(z) = \rho_0^{(s)} erfc[z/(\sqrt{2}\delta)] \tag{5}$$

Here δ is the standard deviation, which is a measure of the surface roughness.

2.2.2 *Kierlik and Rosinberg NLDFT*

Kierlik and Rosinberg (1990) developed an alternative version of nonlocal density functional theory dedicated to mixtures of gases. Therefore it is natural to consider amorphous solid as a component of the binary gas–solid mixture in the framework of the idea of the quenched–annealed system (Ravikovitch and Neimark 2006). The authors called their approach based on extension of the Rosenfeld theory (Rosenfeld 1989) quenched–solid density functional theory (QSDFT). In the case of Kierlik–Rosinberg scheme one can call the approach QSDFT-KR. The excess Helmholtz free energy in this theory is expressed as

$$F_{ex}[\{\rho_i\}] = \int \Phi[\{n_\alpha(\mathbf{r})\}] d\mathbf{r} \tag{6}$$

Here Φ is the excess Helmholtz free energy density of a uniform hard sphere mixture; i is the number of component of the mixture; $n_\alpha(\mathbf{r})$ $(\alpha = 0, 1, 2, 3)$ are weighted densities. The exact expressions for Φ and weighted densities can be found elsewhere (Kierlik and Rosinberg 1990). Like in the NLDFT-AS, the excess Helmholtz free energy is a function of density distributions of solid atoms and adsorbed molecules. Therefore, technically, the application of QSDFT-KR and NLDFT-AS to the gas adsorption on amorphous solids is quite similar.

2.3 Molecular parameters used in the NLDFT versions

There are three molecular parameters of the fluid–fluid interaction, namely, the potential well depth, ε_{ff}, the collision diameter, σ_{ff}, and the hard sphere diameter, d_{HS}. These parameters can be determined at a given temperature with the reference data on the saturation pressure, p_0, the density of liquid, ρ_L at the saturation pressure, and the surface tension, γ. The hard sphere diameter d_{HS} and the group $\varepsilon_{ff}\sigma_{ff}^3$ are easily determined from homogeneous bulk phase properties. To split the group $\varepsilon_{ff}\sigma_{ff}^3$ into ε_{ff} and σ_{ff}, we modeled the vapor–liquid interface in close box (canonical ensemble) having length of $15d_{HS}$. The solid–fluid molecular parameters (ε_{sf} and σ_{sf}) were determined only for the case of argon adsorption on GTCB from the Henry law region of the adsorption isotherm and the Lorenz–Berthelot mixing rule, respectively. We did non need to determine those parameters for the case of argon adsorption on amorphous solids because instead, the whole attractive component of the gas–solid potential was evaluated by the least squares technique. However, in that case the solid atom hard sphere diameter $d_{HS}^{(s)}$ was required. We proceeded from the assumption that $d_{HS}^{(s)}$ should satisfy the requirement of zero value of the excluded volume inside the solid far away from the surface, which is equivalent to the condition

$$\frac{\pi}{6}\left(d_{HS}^{(s)}\right)^3 \rho_0^{(s)} = 1 \tag{7}$$

The values of $\rho_0^{(s)}$ were assumed to be 114 nm^{-3} for non-graphitized carbon black and 66.2 nm^{-3} for silica (accounting only oxygen atoms). This yields 0.2559 nm and 0.3068 nm for the hard sphere diameter of solid atoms in the case of carbon black and silica, respectively. Other molecular parameters are listed in Table 1.

Table 1 Molecular parameters for Ar 87.3 K

	ε_{ff}/k (K)	σ_{ff} (nm)	d_{HS} (nm)	ε_{sf}/k (K)	σ_{sf} (nm)
NLDFT-AS	116.98	0.3317	0.33802	57.650	0.33901
QSDFT-KR	114.14	0.3335	0.33558	–	–

3 Results and discussion

3.1 Adsorption of argon on graphitized carbon black

In this section we consider argon adsorption on graphitized carbon black surface at two temperatures close to N_2 and Ar boiling points. Figure 1 shows experimental Ar adsorption isotherm at 77 and 87.3 K on GTCB Carbopack F having the BET surface area of 6.16 m^2/g (Gardner et al. 2001). Note that the abscissa indicates the absolute pressure. The dashed line is a result of application of the classical Tarazona NLDFT at 87.3 K. One can see from the figure that calculated adsorption isotherm has a prominent shoulder around 100 Pa before the molecular layer completion, whereas the experimental isotherm is quite smooth in

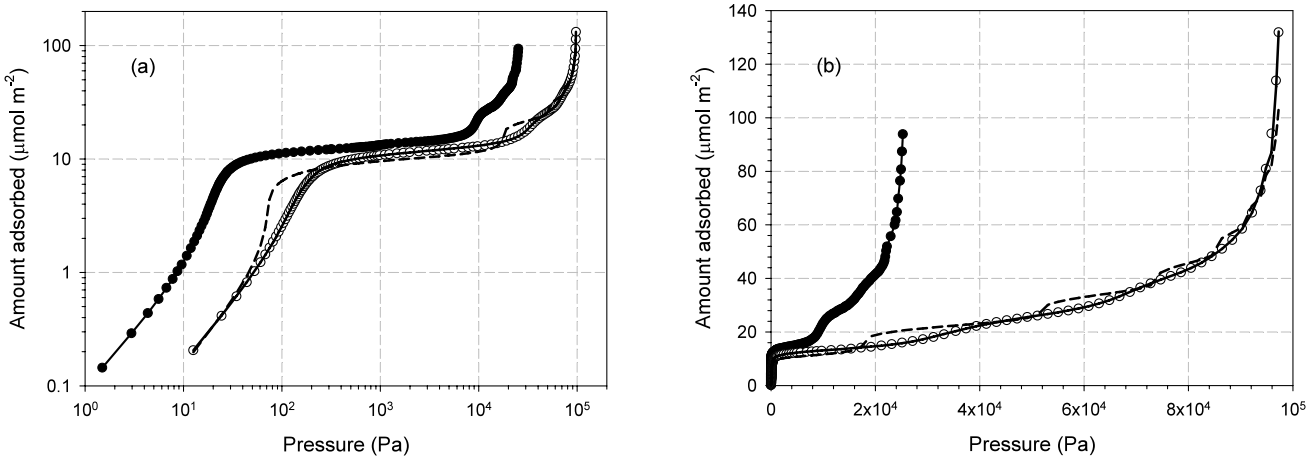

Fig. 1 Argon adsorption isotherm on graphitized carbon black Carbpack F (Gardner et al. 2001) in logarithmic scale (**a**) and linear scale (**b**). Temperature (K): (●) 77, (○) 87.3 K. The *dashed* and *solid lines* corresponding to 87.3 K are plotted with the standard NLDFT and NLDFT with the correction function $j(z)$ (Olivier 1995)

that region. Similar peculiarity is observed in GCMC simulations, which is believed to be due to the effect of polarization of adsorbed molecules, which is not accounted for in the model. One more disappointing deviation from the experimental adsorption isotherm is seen in Fig. 1a in the pressure region between 10^3 and 10^4 Pa (monolayer coverage). This seems insignificant because of the logarithmic scale for loading, but, in fact, NLDFT underestimates the amount adsorbed by about 12%. Of course, this deviation could be reduced by increasing the specific surface area S of the GTCB, but in this case the predicted amount adsorbed would be overestimated in the region of multilayer coverage. In any case, the standard NLDFT fails to describe the experimental isotherm properly. This difficulty can be overcome with the function $j(z)$ introduced by Olivier (1995). We recalculated the function in the region of distance z up to $12d_{HS}$ (Fig. 2) for three values of the specific surface area (m^2/g): 6.16 (S_{BET}), 6.776 ($1.1S_{BET}$), and 7.392 ($1.2S_{BET}$). One can see from the figure that the function $j(z)$ is smaller than unity at a distance smaller than $1.13d_{HS}$, i.e. the intermolecular potential is weakened in this region, presumably due to the polarization effect. Further increase of $j(z)$ in general may reflect either strengthen of the intermolecular interaction, or the entropy drop of the system (i.e. the excess Helmholtz free energy) due to some molecular ordering or 2D solidification. The latter could be a reason why the experimental amount adsorbed at the monolayer coverage exceeds the predicted value. Such an ordering in the system Ar and N_2-graphite surface is indicated with different not only adsorption-based methods (Kjems et al. 1976; Chan et al. 1984; Youn and Hess 1990).

Introducing the correcting function $j(z)$ in the model substantially changes the density distribution of adsorbed

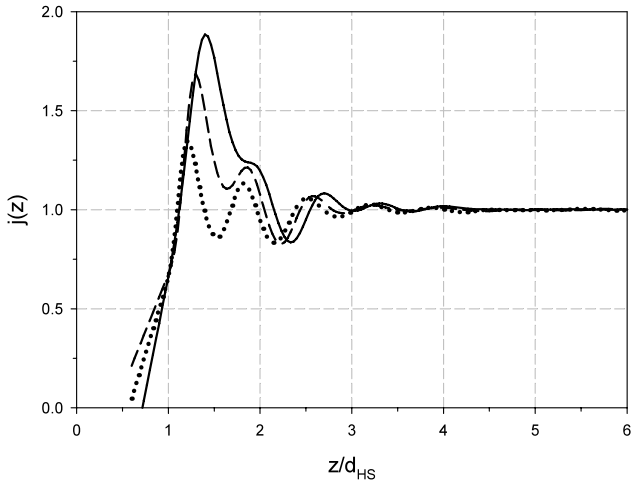

Fig. 2 The function $j(z)$ for the system Ar-GTCB Carbopack F at 87.3 K. The *solid*, *dash*, and *dotted lines* are calculated for the surface area equal to S_{BET}, $1.1S_{BET}$, and $1.2S_{BET}$, respectively. $S_{BET} = 6.16$ m^2/g

argon at the graphite surface. Figure 3 presents Ar density distribution calculated at the saturated pressure and 87.3 K with the original Tarazona NLDFT (Fig. 3a) and accounting for the correcting function for the three values of surface area (Fig. 3b). The ordinate axis indicates the dimensionless density $\rho(z)/\rho_L$, where ρ_L is the bulk liquid density. In the former classical case the adsorbed argon has a prominent layering structure, with the distance between neighboring density peaks being very close to the Ar–Ar collision diameter σ_{ff} ($\approx d_{HS}$). This is expected because a structureless 2D layer exerts a secondary potential field having minimum exactly at a distance of one collision diameter. The situation drastically changes in the latter case of accounting for the function $j(z)$ (Fig. 3b). As is seen from the figure,

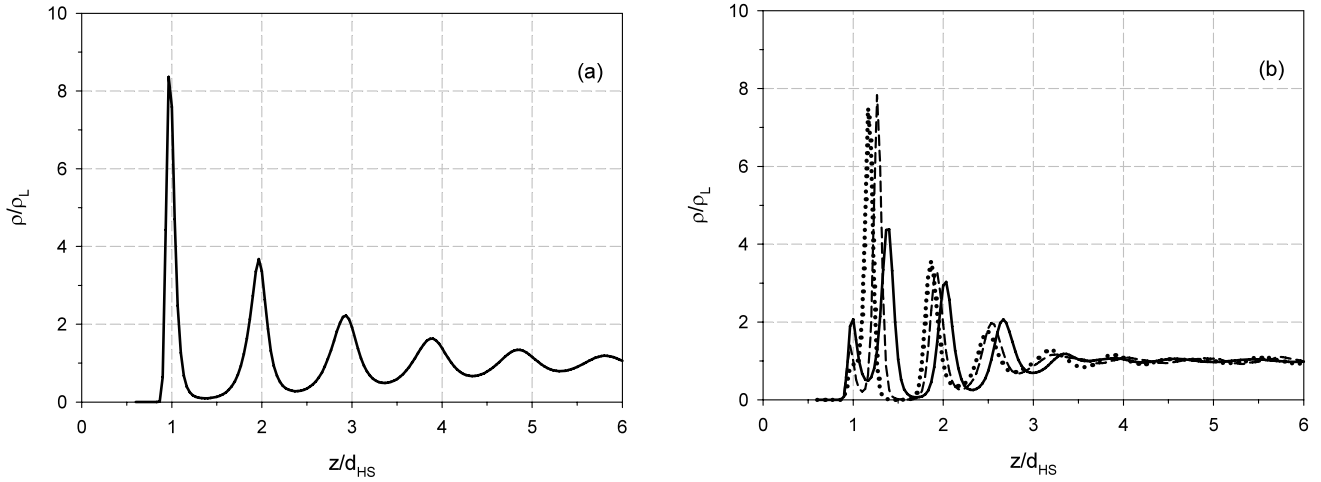

Fig. 3 Density distribution of argon adsorbed on the graphitized carbon black surface Carbopack F at the saturation pressure and 87.3 K calculated with the original Tarazona NLDFT (**a**) and NLDFT accounting for the correcting function $j(z)$ (**b**). Lines are plotted for the same conditions as in Fig. 2

the interlayer distance is much less than the collision diameter. The average interlayer distance over the first five layers is about $0.6\sigma_{ff}$ ($S = S_{BET}$). This points out to a correlated spatial packing of molecules in neighboring layers, which is to some extent associated with the closest packing of hard spheres. As is known, in that case the interlayer distance is $\sqrt{2/3}d_{HS} \approx 0.816d_{HS}$. Besides, the adsorbed phase undergoes the compression due to the external solid–fluid potential having the form of a potential well (the repulsive force acting from the surface is dominant at the position of the first molecular layer, whereas other layers are in the attractive part of the potential field). This is the reason of further reducing of the interlayer distance compared to $0.816d_{HS}$. The increase of the specific surface area compared to S_{BET} leads to the decrease of the adsorbed argon density, making the adsorbed phase closer to the bulk liquid. Indeed, the first and the second density peaks merge into one peak at the surface area enlarged by 20% (the dash-dot line), but the interlayer distance is still markedly less than the collision diameter. The above analysis is not rigorous because any molecular ordering in 2D layers cannot be described with 1D NLDFT model, but nevertheless, the correcting function $j(z)$, being empirical one, does not destroy the basic thermodynamic principle underlying the theory, namely, the condition of minimum of the thermodynamic functional. On the other hand, the function $j(z)$ allows us to quantitatively describe the adsorption isotherm, which is a necessary condition for adequate representation of the adsorption mechanism.

The isosteric heat of adsorption calculated by (4) (the solid line) with two experimental adsorption isotherms measured at 77 and 87.3 K (see Fig. 1), is presented in Fig. 4. In the first molecular layer region the heat of adsorption rises with loading due to the increase of the potential of inter-

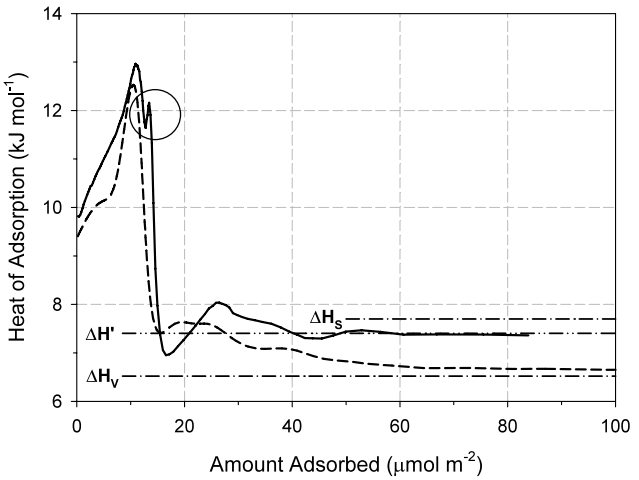

Fig. 4 Isosteric heat of Ar adsorption on GTCB Carbpack F (solid line) at 87.3 K determined from adsorption isotherms at 77.35 and 87.3 K (Gardner et al. 2001) with (4). The *dash line* is plotted with the Tarazona NLDFT and the function $j(z)$. *Lower* and *upper horizontal dash-dot lines* indicate the heat of evaporation, ΔH_V (6.52 kJ/mol), and heat of sublimation, ΔH_S (7.7 kJ/mol), respectively. The *dash-double-dot line* denotes the fictitious heat of phase transition $\Delta H' = 7.40$ kJ/mol (see the text). The *circle* shows the region of 2D phase transition

molecular interaction, which is a commonly known regularity. The onset of formation of the second layer located at a position, where the external potential $V(z)$ is significantly smaller in absolute term compared to the potential minimum, results in the sharp drop of the heat of adsorption, but it is interesting to observe a sudden spike at a loading of 13.4 μmol/g. The same spike was observed in calorimetric measurements of argon and nitrogen adsorption on graphite by Rouquerol et al. (1977). The authors attributed this spike to a degenerated first order phase transition, which confirms

the above semi-quantitative conclusion about the 2D molecular ordering (solidification) above the triple point and coordination in spatial arrangement of molecules in neighboring layers.

The dashed line in Fig. 4 is the prediction with the NLDFT accounting for the correcting function $j(z)$ presented in Fig. 2 for $S = S_{BET}$. The agreement with experimental data seems only fair mainly due to quite large deviations in the multilayer coverage. The predicted isosteric heat of adsorption tends to the heat of evaporation ΔH_V (=6.52 kJ/mol) as expected. On the other hand, the experimental heat determined from two adsorption isotherms with the Clausius–Clapeyron equation asymptotically tends to 7.38 kJ/mol, which is closer to the heat of sublimation ΔH_S (=7.7 kJ/mol) rather than to ΔH_V. However, it does not mean that the adsorbed argon is solidified even in sixth or seventh molecular layer from the graphite surface. It is necessary to take into account that the triple point for argon is 83.78 K which is between the nitrogen and argon boiling points. The dependence of logarithm of the saturated pressure on the inverse temperature is usually very close to the straight line, but this line has a kink at the triple point. It means that the straight line drown trough the two points below and above the triple point would have a slope greater than that corresponding to the vapor–liquid coexistence and smaller than that determined for the vapor–solid region. This gives a fictitious heat of the bulk phase transition $\Delta H'$. In the case of argon the fictitious heat $\Delta H'$ is 7.40 kJ/mol, which completely coincides with the asymptotic heat of adsorption measured experimentally using (4). What this means is that at a distance larger than roughly $3\sigma_{ff}$ from the graphite surface (starting from approximately fifth molecular layer) the adsorbed argon behaves like the bulk condensed phase placed in a weak external potential field, i.e. the adsorbed argon is solid and liquid below and above the triple point, respectively.

3.2 Adsorption of argon on nongraphitized carbon black

The surface of nongraphitized carbon black significantly differs from that of graphite, which usually appears in nonlinear adsorption isotherm at low bulk pressures and a monotone decay of the heat of adsorption with loading. Such a feature is associated with surface heterogeneity and therefore requires application of a distinct approach. In this section we consider adsorption of argon on NGCB Cabot BP 280 graphitized carbon black surface at N_2 (77 K) and Ar (87.3 K) boiling points (Gardner et al. 2001). The BET surface area reported by the authors is 36.25 m^2/g (the average of two values of the BET surface area determined at 77.35 and 87.3 K). The isotherms are depicted in Fig. 5. For comparison the dashed and dash-dot lines in the figure present Ar adsorption isotherms on GTCB Carbopack F at the same

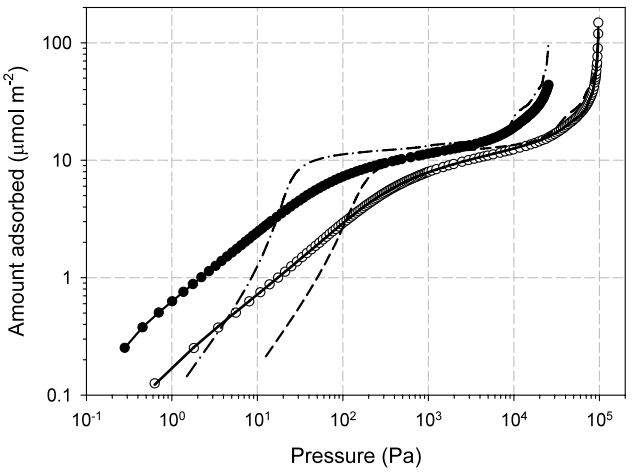

Fig. 5 Argon adsorption isotherms on nongraphitized carbon black Cabot BP 280 (Gardner et al. 2001) at 77 (●) and 87.3 K (○). The *solid line* at 87.3 K is calculated with the NLDFT-AS approach. The *dash-dot* and the *dashed line* are adsorption isotherms of argon on GTCB at 77 and 87.3 K, respectively

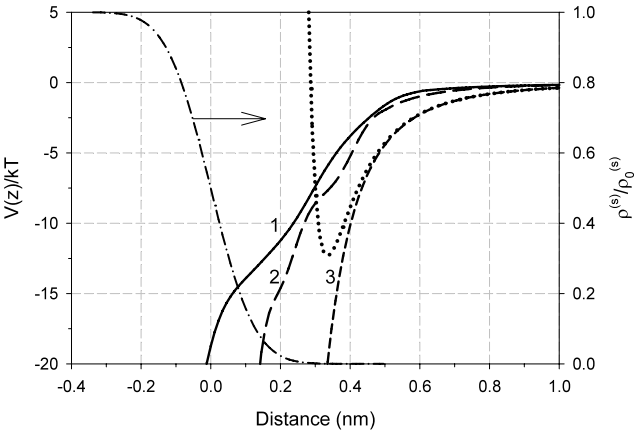

Fig. 6 The attractive solid–fluid potential in the system Ar-NGCB Cabot BP 280 determined with Ar adsorption isotherm at 87.3 K using NLDFT-AS (*1*) and QSDFT-KR (*2*) models. The *dotted line* is the 10-4-3 Steele potential defined for the graphite surface, and the *short-dash line* (*3*) is the attractive component of the potential. The *dash-dot line* shows the change of the carbon atom density across the diffuse surface zone at the standard deviation of 0.1 nm

temperatures. One can see that the slope of the isotherms in the case of NGCB is much smaller in the low pressure range compared to that for the smooth graphite surface, i.e. the Henry law region is absent. This is a consequence of energetic heterogeneity of NGCB due to surface defects, broken bonds, functional groups, etc. Because of complexity of the surface structure, it is hard to predict the solid–fluid potential like in the case of graphite surface. For this reason we determined the potential directly from the adsorption isotherm of argon at 87.3 K. The attractive component of the potential determined with the NLDFT-AS (1) and QSDFT-KR (2) is presented in Fig. 6. The repulsive component of

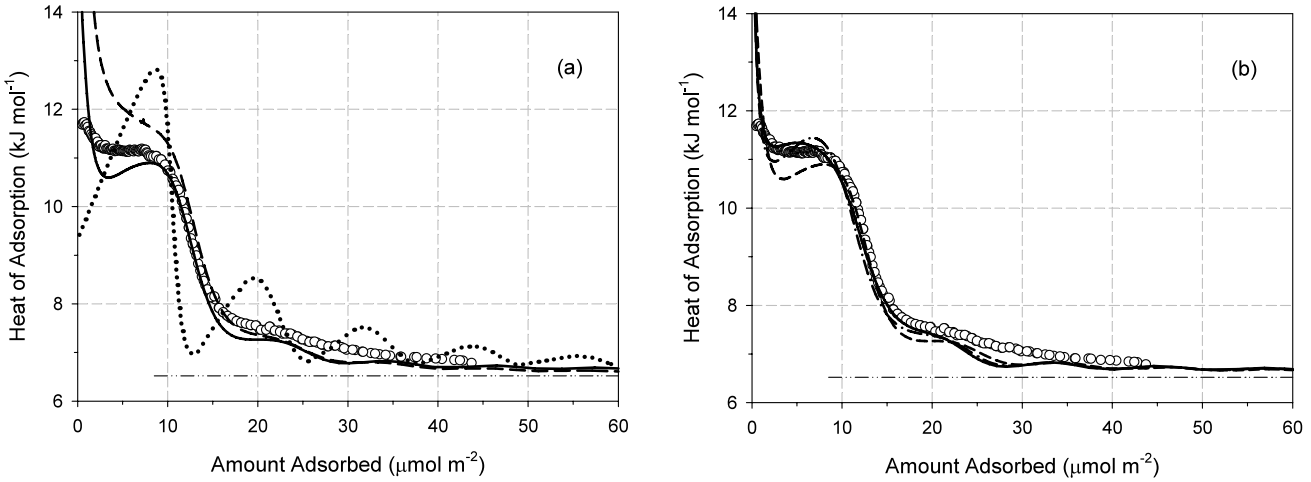

Fig. 7 Isosteric heat of argon adsorption q_{st} on carbon black Cabot BP 280. *Symbols* denote experimental points determined with (4) from adsorption isotherms measured at 77 and 87.3 K. Section (**a**) shows a comparison of the experimental dependence of q_{st} on amount adsorbed with those predicted with NLDFT-AS (—) and QSDFT-KR (– – –) at the standard deviation $\delta = 0.1$ nm. The *dotted line* is for the standard Tarazona NLDFT. Section (**b**) shows the effect of surface roughness on the heat of adsorption calculated with NLDFT-AS model. δ (nm): 0.1 (– – –), 0.15 (· · ·), 0.2 (—). The *horizontal dash-double-dot line* denotes the heat of evaporation

the potential (not shown in figure) is modeled via the excess Helmholtz free energy. Calculations were carried out at a surface roughness corresponding to the standard deviation δ of 0.1 nm (5). The dash-dot line represents the carbon atom density profile across the NGCB surface. It is interesting to compare the determined potentials with the attractive component of the 10-4-3 Steele potential defined for the graphite surface (3). One can see that in the case of nongraphitized carbon black the potential shifts toward the surface. The reason is the surface roughness and disordered nature of an amorphous surface having troughs and convexities, which in average allows molecules to approach closer to the surface. This also extends the potential over a larger distance normal to the surface. In this context it should be emphasized, however, that a quantitative description of a gas adsorption on amorphous solid is impossible in the framework of the conventional NLDFT by adjusting the solid–fluid potential. The peculiarity of the density functional theory versions developed for the amorphous solids is that the repulsive component of the solid–fluid potential increases with the amount adsorbed, which reduces the total potential in absolute term with loading and thereby models the energetic heterogeneity of the surface (Ustinov et al., 2005, 2006, 2007).

The isosteric heat of adsorption for the system under consideration determined from the two adsorption isotherms using (4) is presented in Fig. 7. An important feature of the experimental heat-loading dependence is that q_{st} asymptotically tends to the heat of evaporation ΔH_V, rather than to the fictitious heat of phase transition $\Delta H'$ like in the case of argon adsorption on the graphitized carbon black. What this means is that even at a large distance from the surface the adsorbed argon is liquid-like both at 87.3 and 77 K despite in the latter case the temperature is below the argon triple point (83.78 K). This suggests that surface defects hamper formation of a long-range molecular ordering inherently related to crystalline solids. Figure 7a shows results of application of our extension of the Tarazona smoothed density approximation to amorphous solids, NLDFT-AS (the solid line) and the Kierlik–Rosinberg QSDFT version (the dashed line). Both models fit the experimental dependence fairly well. For comparison, the dotted line presents the heat of adsorption calculated with the standard Tarazona NLDFT developed for smooth crystalline surfaces. It is clear that in the latter case the theory does not reflect the adsorption mechanism on the rough surface. It should be noted that the theoretical heat of adsorption is predicted from the single isotherm and is not a result of any adjustment. However, some discrepancy is observed in the monolayer region, with both models developed for amorphous surfaces substantially overestimating the heat of adsorption at a very small amount adsorbed. It is quite possible that such a deviation is somehow associated with localized adsorption at extremely low loading, which requires application of an alternative approach. Anyway, the NLDFT-AS fits the heat of adsorption markedly better than the QSDFT-KR does. Furthermore, the fitting can be improved by a proper adjustment of the standard deviation δ. The effect of δ on the isosteric heat of adsorption is shown in Fig. 7b. One can see that the best fit (the solid line) corresponds to the standard deviation of 0.2 nm, which seems to be a quite realistic value. In the case of QSDFT-KR the situation is worse because the predicted heat of adsorption always overestimates experimental values in the region of monolayer coverage.

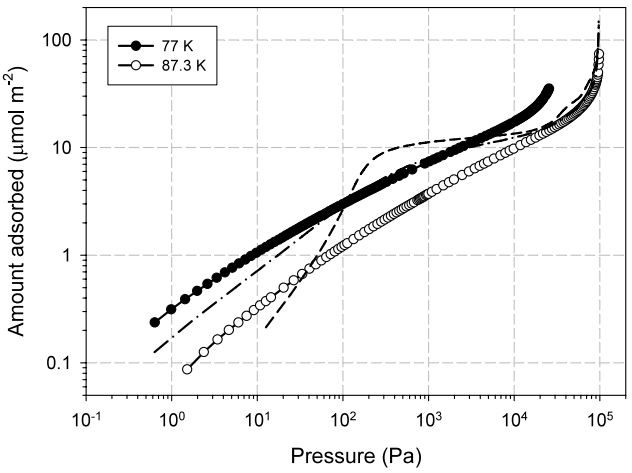

Fig. 8 Argon adsorption isotherm on LiChrospher-Si-1000 surface at 77 K (Kruk and Jaroniec 2002) and 87.3 K (Kruk and Jaroniec 2000). The BET surface is taken as 19.65 m^2/g. The *dashed* and the *dash-dot line* are drawn for argon adsorption at 87.3 K on Carbopack F and Cabot BP 280, respectively

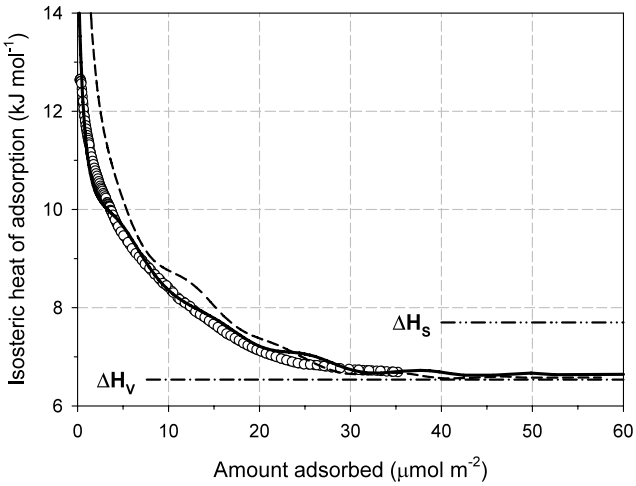

Fig. 9 Isosteric heat of Ar adsorption on the nonporous silica at 87.3 K. The *solid line* is calculated with NLDFT-AS for the standard deviation δ of 0.2 nm. The *dashed line* is predicted by the QSDFT-KR for $\delta = 0.1$ nm

3.3 The system Ar-nonporous silica

Nonporous silica is a typical representative of amorphous solids. In this section we consider argon adsorption on the LiChrosper-Si-1000 sample (Kruk and Jaroniec, 2000, 2002). The isotherms of argon, as in the previous cases, are presented on logarithmic scales at 77 and 87.3 K in Fig. 8. The comparison of argon adsorption isotherms on the graphitized carbon black, nongraphitized carbon black, and silica shows that in the latter case the surface is especially heterogeneous, which is confirmed by the experimental dependence of the heat of adsorption on amount adsorbed (Fig. 9) determined with (4). It is seen from the figure that q_{st} sharply decreases with loading approaching the heat of evaporation. Like in the case considered in the previous section, this indicates that adsorbed argon at 77 K behaves similar to supercooled bulk liquid, because otherwise the heat of adsorption determined with (4) would be inevitably equal to the fictitious value 7.4 kJ/mol. In our previous work (Ustinov et al. 2005) we came to the same conclusion in a different way. We determined the solid–fluid potential from the adsorption isotherm at 87.3 K and than predicted the isotherm at 77 K. It turned out that if one takes the true saturation pressure p_0 of 25.49 kPa corresponding to the vapor–solid coexistence, the predicted isotherm matches the experimental data rather poorly. However, having replaced that value by the saturated pressure of supercooled liquid argon at 77 K, namely 29.32 kPa, the fitting became excellent.

The solid line in Fig. 9 is calculated with the NLDFT-AS model at the standard deviation δ of 0.2 nm. As in the case of NGCB, this value provides the best fit of the heat–amount adsorbed dependence. One can see that the predicted curve excellently fits the experimental data, whereas the QSDFT-KR substantially overestimates q_{st}, especially at low loading.

To summarize, the study performed for argon adsorption on three types of surface coupled with the analysis of the heat of adsorption has confirmed a good descriptive ability of the approach based on extending the classical nonlocal density functional theory to amorphous solids like nongraphitized carbon black and nonporous silica. The possibility of quantitative reproducing the isosteric heat of adsorption seems especially promising and allows deeper insight into the mechanism of adsorption and justifies further investigations.

4 Conclusion

We have coherently analyzed argon adsorption on smooth and rough heterogeneous surfaces using the Tarazona and Kierlik–Rosinberg versions of density functional theory and its modifications for the case of amorphous solids. In the case of graphitized carbon black, the use of the Olivier correcting function $j(z)$ allowed us to quantitatively describe the adsorption isotherm, but drastically changed the density distribution of argon at the surface. It turned out that the layer-to-layer distance in the adsorbed phase at a high loading is of about 0.6 the collision diameter indicating a highly ordered and mutually coordinated structure of molecular layers. The sharp spike on the isosteric heat curve just after the completion of the first monolayer also suggests the first order 2D phase transition. At the same time, the behavior of the adsorbed argon at a distance larger than about three collision diameters from the graphite surface seems to

be completely the same as that of the bulk phase. Contrary to that, argon adsorbed on a defected surface like that of nongraphitized carbon black and silica behaves like a supercooled liquid even at a very large distance from the surface available in our analysis. We have shown that nonlocal density functional theory extended to amorphous surfaces excellently fits experimental adsorption isotherms and, most importantly, allows well approximating of the isosteric heat of adsorption. Moreover, the NLDFT-AS developed in our previous works is able to quantitatively reproduce the heat of adsorption by adjusting the parameter δ (the standard deviation in (5)), which is a measure of the surface roughness.

Acknowledgement Support from the Russian Foundation for Basic Research is gratefully acknowledged (project 06-03-32268-a).

References

Chan, M.H.W., Migone, A.D., Miner, K.D., Li, Z.R.: Thermodynamic study of phase transitions of monolayer N_2 on graphite. Phys. Rev. B **30**, 2681–2694 (1984)

Do, D.D., Do, H.D.: Effects of quadrupole moments of graphite surface on adsorption of simple gases on graphitized thermal carbon black. Colloids Surf. A Physicochem. Eng. Aspects **300**, 50–59 (2007)

Do, D.D., Do, H.D., Kaneko, K.: Effect of surface perturbed intermolecular interaction on adsorption of simple gases on a graphitized carbon surface. Langmuir **20**, 7623–7629 (2004)

Gardner, L., Kruk, M., Jaroniec, M.: Reference data for argon adsorption on graphitized and nongraphitized carbon blacks. J. Phys. Chem. B **105**, 12516–12523 (2001)

Kierlik, E., Rosinberg, M.L.: Free-energy density functional for the inhomogeneous hard-sphere fluid: application to interfacial adsorption. Phys. Rev. A **42**, 3382–3387 (1990)

Kjems, J.K., Passel, L., Taub, H., Dash, J.G., Novaco, A.D.: Neutron scattering study of nitrogen adsorbed on basal-plane-oriented graphite. Phys. Rev. B **13**, 1446–1462 (1976)

Kruk, M., Jaroniec, M.: Accurate method for calculating mesopore size distributions from argon adsorption data at 87 K developed using model MCM-41 materials. Chem. Mater. **12**, 222–230 (2000)

Kruk, M., Jaroniec, M.: Determination of mesopore size distributions from argon adsorption data at 77 K. J. Phys. Chem. B **106**, 4732–4739 (2002)

Neimark, A.V., Ravikovitch, P.I., Grün, M., Schüth, F., Unger, K.K.: Pore size analysis of MCM-41 type adsorbents by means of nitrogen and argon adsorption. J. Colloid Interface Sci. **207**, 159–169 (1998)

Olivier, J.P.: Modeling physical adsorption on porous and nonporous solids using density functional theory. J. Porous Mater. **2**, 9–17 (1995)

Olivier, J.P., Conklin, W.B., Szombathely, M.V.: Determination of pore size distribution from density functional theory: a comparison of nitrogen and argon results. Stud. Surf. Sci. Catal. **87**, 81–89 (1994)

Ravikovitch, P.I., Neimark, A.V.: Density functional theory model of adsorption on amorphous and microporous silica materials. Langmuir **22**, 11171–11179 (2006)

Rosenfeld, Y.: Free-energy model for the inhomogeneous hard-sphere fluid mixture and density functional theory of freezing. Phys. Rev. Lett. **63**, 980–983 (1989)

Rouquerol, J., Partyka, S., Rouquerol, F.: Calorimetric evidence for a bidimensional phase change in the monolayer of nitrogen or argon adsorbed on graphite at 77 K. J. Chem. Soc. Faraday Trans. **73**, 306–314 (1977)

Tarazona, P.: Free-energy density functional for hard spheres. Phys. Rev. A **31**, 2672–2679 (1985)

Tikhonov, A.N., Arsenin, V.Y.: Solutions of Ill-Posed Problems. Wiley, New York (1977)

Ustinov, E.A., Do, D.D.: Non-additivity of attractive potentials in modeling of N_2 and Ar adsorption on graphitized carbon black and porous carbon by means of density functional theory. Part. Part. Syst. Characteriz. **21**, 161–169 (2004)

Ustinov, E.A., Do, D.D., Jaroniec, M.: Application of density functional theory to equilibrium adsorption of argon and nitrogen on amorphous silica surfaces. Appl. Surf. Sci. **252**, 548–561 (2005)

Ustinov, E.A.: Do, D.D., Jaroniec, M.: Features of nitrogen adsorption on nonporous carbon and silica surfaces in the framework of classical density functional theory. Langmuir **22**, 6238–6244 (2006)

Ustinov, E.A.: Do, D.D., Fenelonov, V.B.: Modeling of heterogeneous surfaces and characterization of porous materials by extending density functional theory for the case of amorphous solids. Appl. Surf. Sci. **253**, 5610–5615 (2007)

Weeks, J.D., Chandler, D., Andersen, H.C.: Role of repulsive forces in determining the equilibrium structure of simple liquids. J. Chem. Phys. **54**, 5237–5247 (1971)

Youn, H.S., Hess, G.B.: Reentrant first-order layering transition in multilayer argon films on graphite. Phys. Rev. Lett. **64**, 918–921 (1990)